Stanford Exploration Project, Report 77, November 17, 1997, pages 273–290

Stanford Exploration Project, Report 77, November 17, 1997, pages 273–290

Lateral prediction techniques: FX-decon versus two-D deconvolution

Ray Abma[1]

keywords: *deconvolution, two-dimensional, noise, filtering*

ABSTRACT

The results of two-dimensional lateral deconvolution are similar to those of FX-decon, however, two-dimensional lateral deconvolution produces less artificial lineup in noise than FX-decon. Modifying the filter shape in two-dimensional deconvolution may allow more control over the process than is allowed in FX-decon.

INTRODUCTION

In seismic exploration, predictions are used along both the time and space axis of seismic sections, but the applications of these predictions are different. Along the time axis, the desired output is the unpredictable part of the trace. The predicatable part contains the source wavelet and multiple reflections that reduce the apparent resolution. Along the spatial axis the desired output is the predictable part of the traces, and the unpredictable part is often noise that doesn't correlate between traces. While this lateral prediction is understandable in a simple layered earth, even a subsurface made up of random scatterers produces lateraly continuous diffraction events in unmigrated sections.

FX-decon is a useful noise-attenuation technique that has become a standard seismic processing tool. As introduced by Canales(1984), it predicts linear events with a complex least-squares prediction technique in the frequency-space domain.

The two-dimensional deconvolution discussed here uses the routines developed by Claerbout and shown in the references (Claerbout, 1992) and in(Claerbout, 1992b). These routines calculate filters using a conjugate-gradient method directly from the data in the time-space domain rather than Fourier transforming the data before doing the predictions.

Where FX-decon does a spatial prediction for each frequency, the two-dimensional deconvolution calculates a single filter. Although the number of coefficients in the

[1]**email:** not available

filter is typically greater for two-dimensional deconvolution than for FX-decon, FX-decon creates a different filter for each frequency. Thus, two-dimensional deconvolution is more constrained than FX-decon in making its predictions.

In this paper, the two-dimensional deconvolution differs from Claerbout's work by extending the filter in the x-direction and limiting it in the time-direction. Where Claerbout was trying to predict single plane waves, I am attempting to predict anything that is laterally predictable with a reasonably small two-dimensional filter. We hope that the two-dimensional deconvolution allows more control over the filter action by modifying the filter shape.

I show that two-dimensional deconvolution and FX-decon produce similar results for most cases. It appears that two-dimensional deconvolution's advantage is that it does not line up noise as much as FX-decon when no predictable signal is present. Also, two-dimensional deconvolution does not produce the artificial lineups along strong signals to the extent FX-decon does.

FX-DECON

FX-decon is a simple process that predicts linear events by making predictions in the frequency-space domain.

The FX-decon prediction process depends on the form of linear events in frequency versus x, x being the space direction. Given a linear event, $f(x) = \delta(a + bx - t)$, the Fourier transform of this event is $f(\omega) = e^{i\omega(a+bx)}$ or $f(\omega) = e^{i\omega a}(\cos(\omega bx) + i\sin(\omega bx))$. In x, the function is clearly periodic. To predict a linear event, a least squares prediction filter is calculated, using $f = (X^\dagger X)^{-1} X^\dagger d$ where f is the prediction filter, d is the desired output, and X is a matrix filled with shifted versions of the input series in x. $\dagger$ indicates the transpose conjugate.

Following the nomenclature of Gulunay(1986), d is the data shifted by one sample, or $d = (\; x_2 \quad x_3 \quad \cdots \quad x_n \quad x_{n+1} \;)$. The input data, $(\; x_1 x_2 \quad x_3 \quad \cdots \quad x_n \;)$, forms the matrix X below:

$$X = \begin{pmatrix} x_1 & 0 & 0 & 0 & \cdots & 0 & 0 \\ x_2 & x_1 & 0 & 0 & \cdots & 0 & 0 \\ x_3 & x_2 & x_1 & 0 & \cdots & 0 & 0 \\ . & . & . & . & . & . & . \\ . & . & . & . & . & . & . \\ . & . & . & . & . & . & . \\ x_n & x_{n-1} & x_{n-2} & x_{n-3} & x_{n-4} & x_{n-5} & \cdots \\ 0 & x_n & x_{n-1} & x_{n-2} & x_{n-3} & x_{n-4} & \cdots \\ 0 & 0 & x_n & x_{n-1} & x_{n-2} & x_{n-3} & \cdots \\ . & . & . & . & . & . & . \\ . & . & . & . & . & . & . \\ . & . & . & . & . & . & . \\ 0 & 0 & 0 & 0 & \cdots & 0 & x_n \end{pmatrix}, \tag{1}$$

X being a matrix of size $(2n-1)$ by n. While d may be built with a longer shift, a shift of one sample is typically used.

The process of applying FX-decon starts by partitioning the data into windows small enough so events of interest appear linear. The data within each window are then Fourier transformed. For each frequency, a prediction filter is calculated and applied twice; once forward in space and once backwards. The two predictions are summed, the inverse Fourier transform applied, and the windows merged back into the output. Note that the operations within each frequency are independent of other frequencies. This allows a large degree of freedom in the prediction of the output.

Another interesting feature of the FX-decon process pointed out by Spitz (1991) involves the relationships of the response of a dip at one frequency to that at another frequency. In Figure 1, a single dipping event is shown in time and after Fourier transformation of the time axis. It can be seen that the events are periodic both in frequency and in space. The periodicity at low frequency may be used to predict the shape of the higher frequency components and may be used to guide interpolation of events that are aliased in the high frequency components, but not aliased at low frequencies.

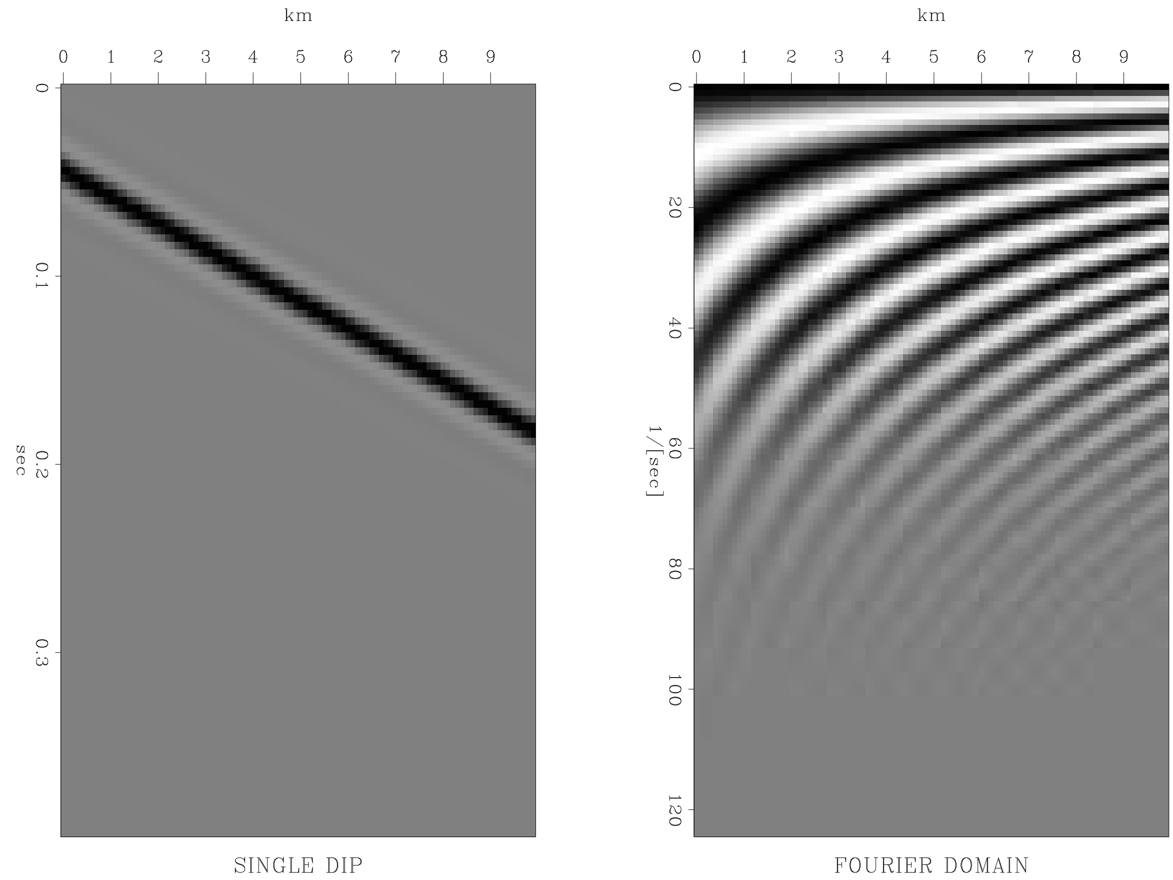

Figure 1: A single dip in the time domain and in the Fourier domain. The real part after Fourier transformation in time is shown. $\boxed{\text{ray1-sdip}}$ [ER]

TWO-D DECONVOLUTION FILTERING

Two-dimensional deconvolution creates a filter that minimizes the energy in a window using a least squares criteria. The filters used in the examples in this article have a form similar to the one below:

$$\begin{array}{ccccc} \cdot & a_{12} & a_{13} & a_{14} & a_{15} \\ \cdot & a_{22} & a_{23} & a_{24} & a_{25} \\ 1 & a_{32} & a_{33} & a_{34} & a_{35} \\ \cdot & a_{42} & a_{43} & a_{44} & a_{45} \\ \cdot & a_{52} & a_{53} & a_{54} & a_{55} \end{array} \tag{2}$$

The vertical axis is the time axis, and the horizontal axis is the space axis. For clarity, "$\cdot$"s are used to indicate zeros.

While the size of this filter may be modified to match the desired output, generally I've found three coefficients in the time direction are sufficient unless steep dips are found. The number of coefficients in the space direction may depend on how many dips occur within the window and how much prediction is desired. The filter coefficients are calculated using a conjugate-gradient technique described in Claerbout(1992).

One advantage of the two-dimensional deconvolution approach to lateral prediction is that the shape of the filter can be modified to match the range of dips desired. As an example, the filter below might be used to predict a range of low-angle dips:

$$\begin{array}{ccccc} \cdot & \cdot & \cdot & \cdot & a_{15} \\ \cdot & \cdot & a_{23} & a_{24} & a_{25} \\ 1 & a_{32} & a_{33} & a_{34} & a_{35} \\ \cdot & \cdot & a_{43} & a_{44} & a_{45} \\ \cdot & \cdot & \cdot & \cdot & a_{55} \end{array} \tag{3}$$

To keep the calculation and application of the filter symmetrical, the two-dimensional deconvolution examples shown in this paper have two filters calculated and applied for each window: one forward in space and one reversed. In the program used here, the filter is not extended beyond times where a full filter response is available, so the two-dimensional deconvolution results shown have the original data at the top and bottom of the section.

Two-dimensional deconvolution uses only two filters within each window, compared to FX-decon, which uses a separate filter for each frequency. While the two-dimensional deconvolution filter will have more coefficients than each filter used in the FX-decon, the FX-decon will have a different filter for each frequency. Thus, the two-dimensional deconvolution filter is much more constrained in predicting events than FX-decon. The computer time needed to apply these two processes are comparable, since the many filters calculated by FX-decon are very short and the one filter calculated by the two-dimensional deconvolution is longer. Since the time to calculate a filter is proportional to n^2, where n is the number of filter coefficients, the calculation times used by the two approaches are about equal.

The similarity of the results of two-dimensional deconvolution and FX-decon may be explained by the similarity of the two filters in the time domain. If the FX-decon filters are collected and transformed into the space-time domain, they will transform into a filter that appears similar to Filter (3), but having more rows. The number of rows will be the number of time samples in the window, giving the FX-decon a long effective length in time. This extended length in time allows the FX-decon to create false lineups if the time-domain representation of the FX-decon operator has coefficients of significant strength far from the output point. For a more complete comparison of the two filters see (Abma and Claerbout, 1993) in this volume.

EXAMPLES

A simple two-dip example shows that both FX-decon and two-dimensional deconvolution retain the original signal. Figure 2 and Figure 3 compare the results of two-dimensional deconvolution and FX-decon in the noiseless case. The weak events seen in the difference sections are the result of the sampling used in creating the dipping events. Flat events may be completely removed using either of these techniques.

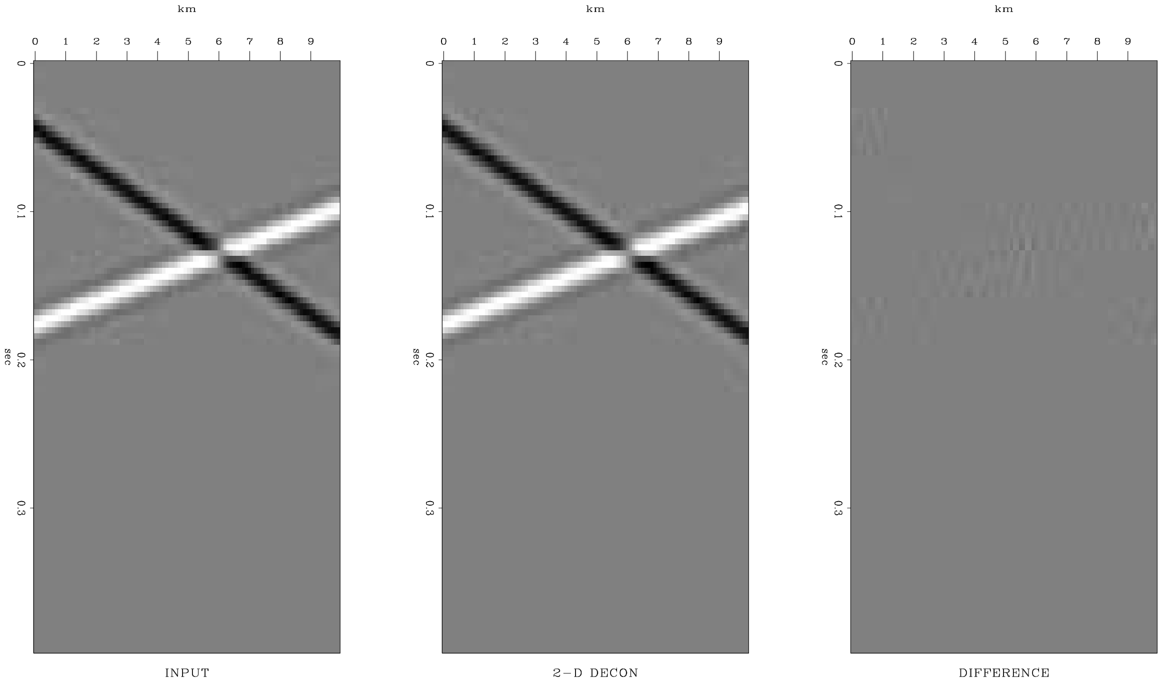

Figure 2: Two-D prediction-error filtering $\boxed{\text{ray1-dips}}$ [ER]

When noise is added, FX-decon and two-dimensional deconvolution show similar results, as seen in Figures 4 and 5. The noise is significantly attenuated, and the linear events are retained. Notice that the two-dimensional deconvolution removes

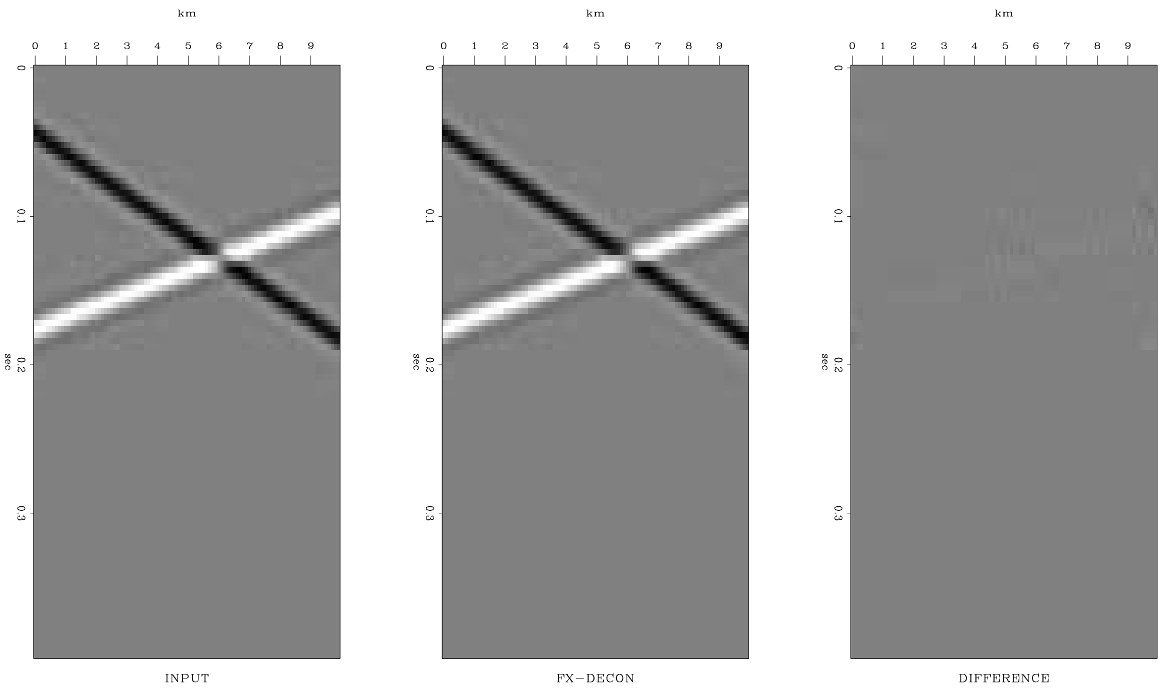

Figure 3: FX-decon filtering ray1-dipsfx [ER]

more noise than FX-decon in the lowest window where no signal is present. Three windows in time and four windows in x with fifty percent overlap are used in Figures 4 and 5. The noise remaining at the top and bottom of the prediction section of Figure 4 is the original data, since the output is not predicted unless the filter covers a full set of data. This may be remedied by saving the filter after it is calculated and then applying it to a wider range of data. In this version of the two-dimensional deconvolution program, the calculation of the filter and the filtering is performed simultaneously.

Both processes applied to real data again show that the results are similar, as seen in Figures 6 and 7. In the shallow section, both filters have predicted the even-odd effect, where alternate traces have different amplitudes, since both filters can predict it. There were 16 overlapping windows in time and three windows in x in these examples.

The previous similarities between the processes are seen in the global image of a portion of a dataset created by Shearer(1991) seen in Figures 8 and 9. Notice that there is some lineup of the noise with strong events in Figure 9. Otherwise, the FX-decon appears to do as well as two-dimensional deconvolution. A comparison using the full dataset is shown in Figure 10.

More significant differences are seen when 2-dimensional deconvolution and FX-decon are applied to random noise. The predictions shown by Figures 11 and 12 are seen to have lined up some of the random noise, but the FX-decon has left more

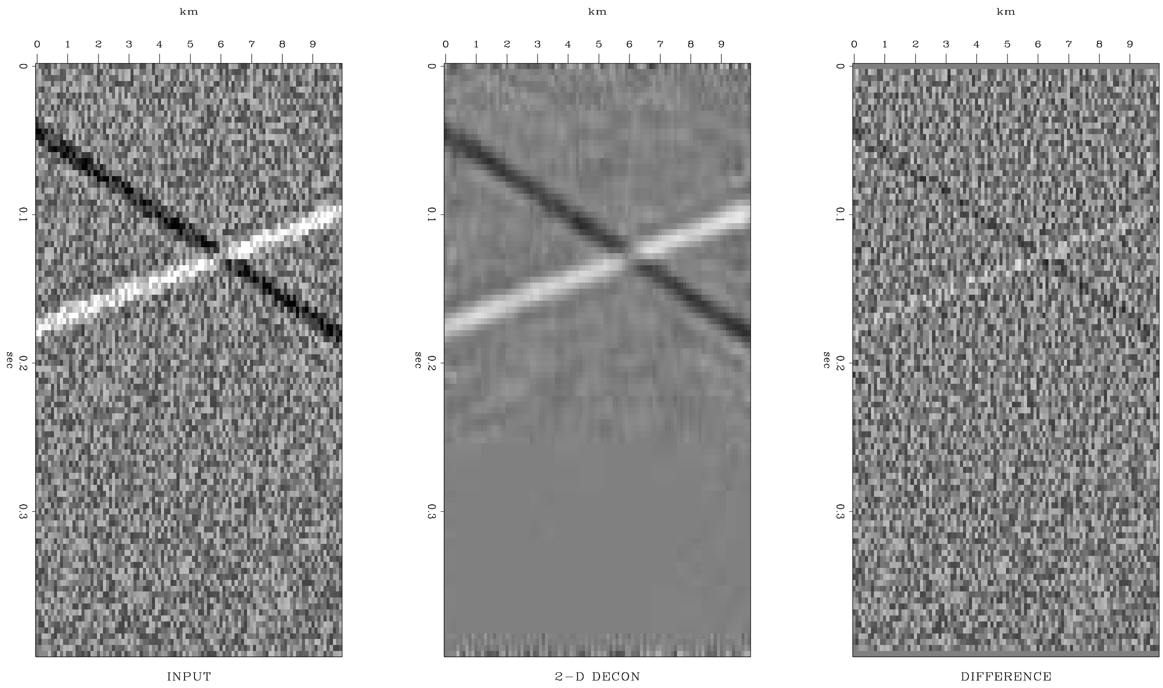

Figure 4: Two-D prediction-error filtering. Notice how weak the noise is on the lower part of the output compared to Figure 5. The original data are output at the top and bottom because the filters have not been applied past the edges there. ray1-noise [ER]

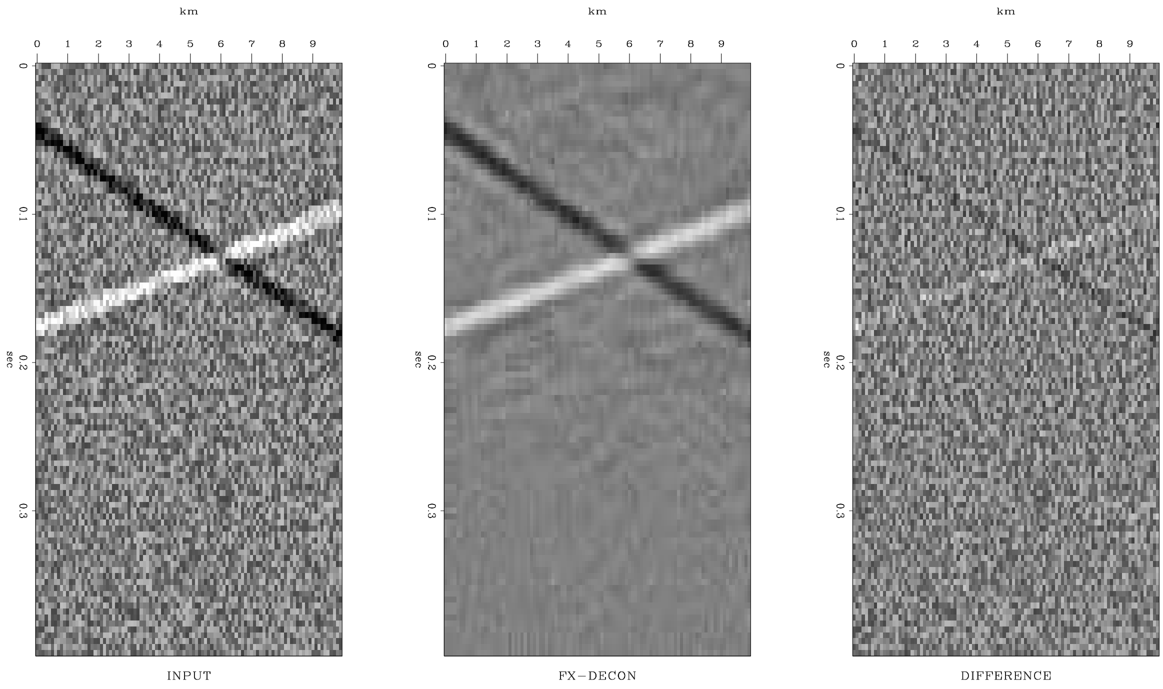

Figure 5: FX-decon filtering. Notice how strong the noise is on the lower part of the output compared to Figure 4. ray1-noisefx [ER]

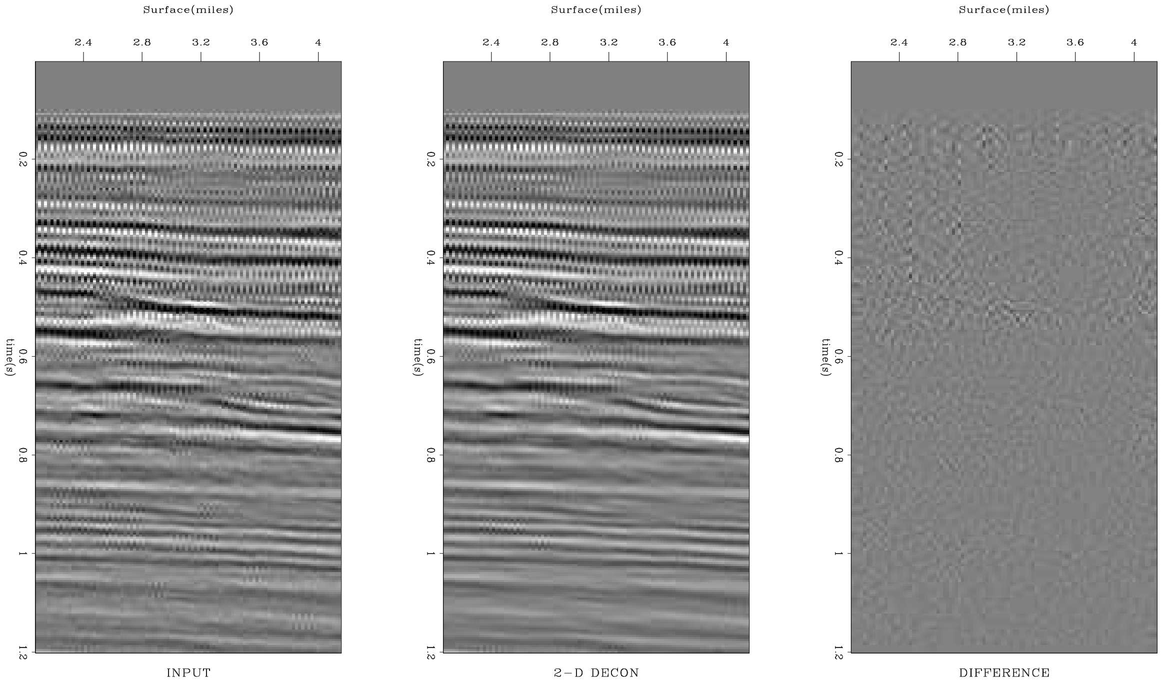

Figure 6: Two-D prediction-error filtering applied to a Gulf of Mexico line. ray1-WGstack [ER]

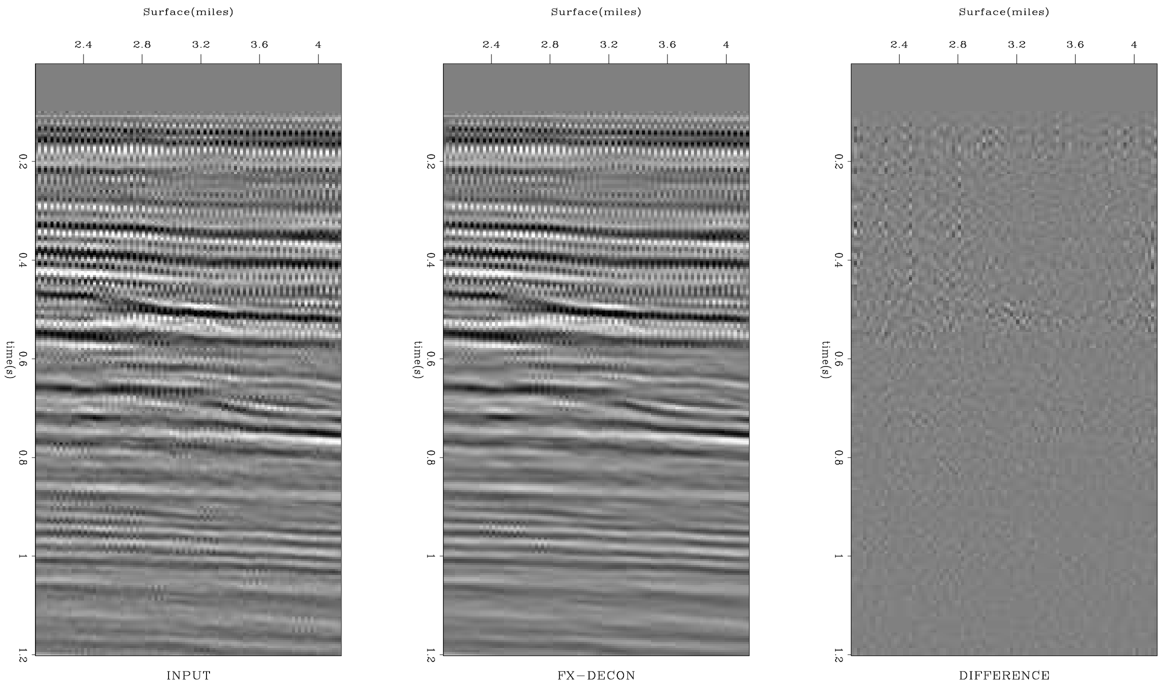

Figure 7: FX-decon filtering applied to a Gulf of Mexico line. ray1-WGstackfx [ER]

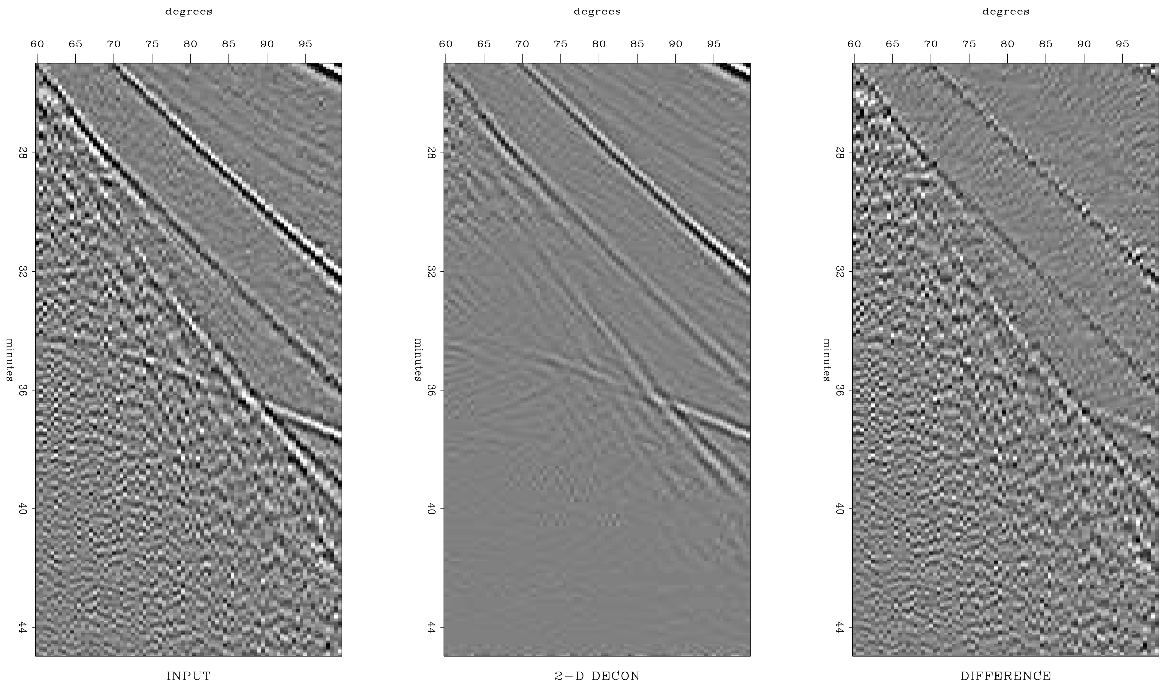

Figure 8: Two-D deconvolution filtering of the horizontal component of Shearer's global image dataset. There is less ringing here than in Figure 9. ray1-transverse [ER]

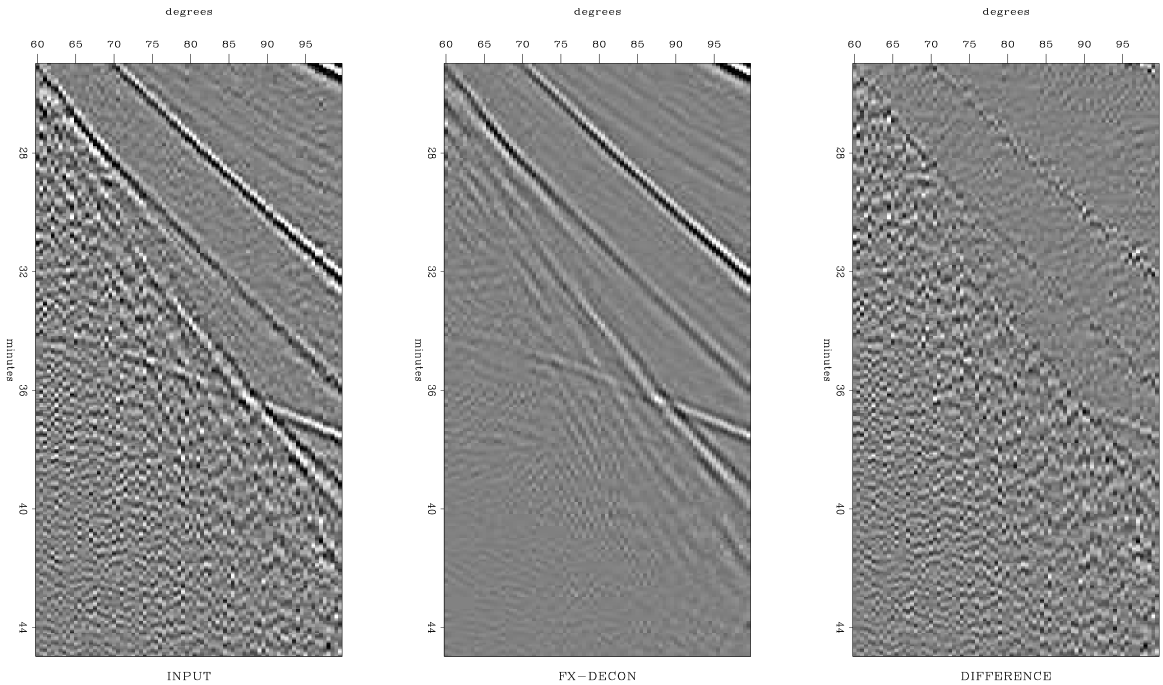

Figure 9: FX-decon filtering of the horizontal component of Shearer's global image dataset. There is more ringing here than in Figure 8. ray1-transversefx [ER]

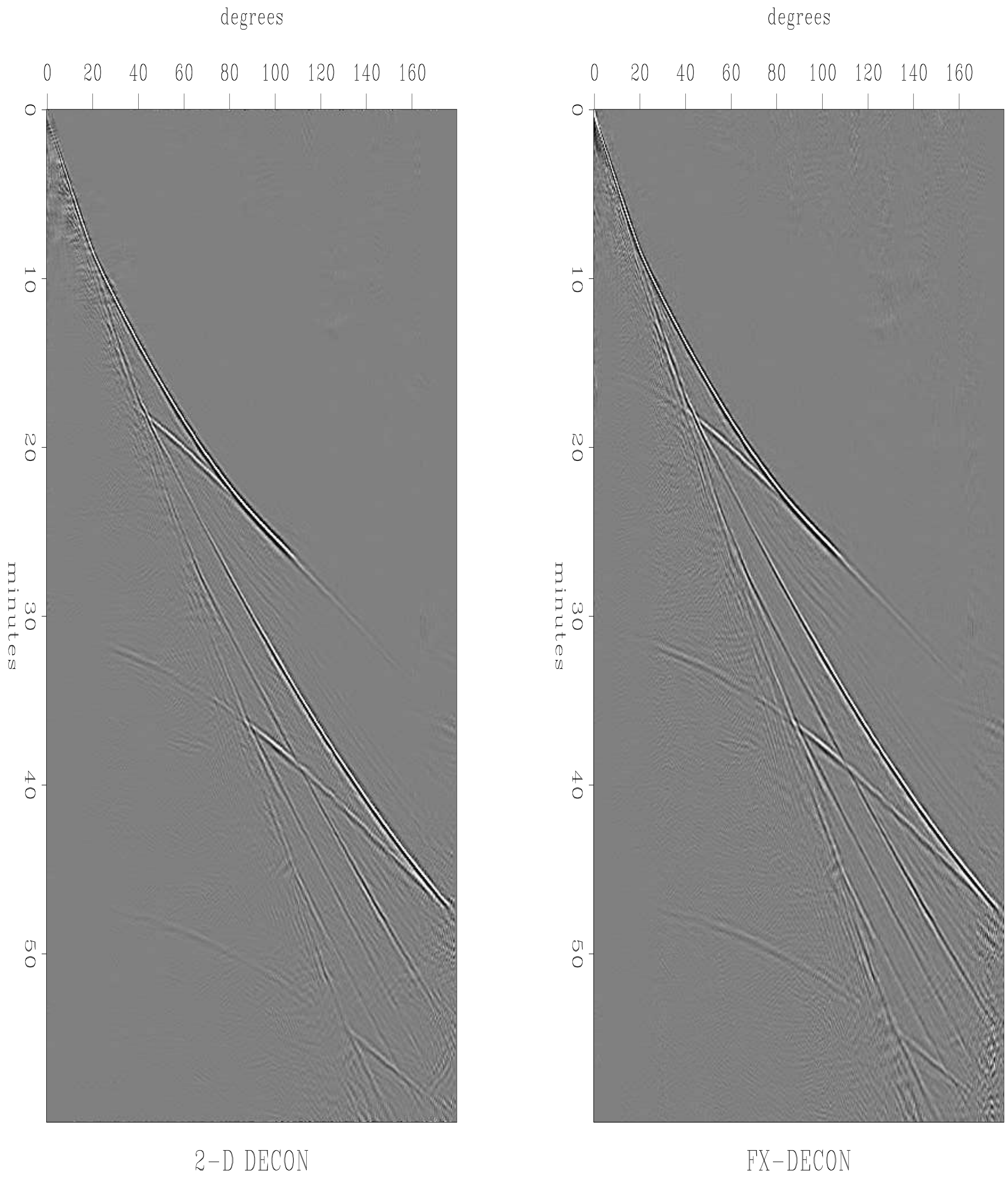

Figure 10: Two-D deconvolution and FX-decon of the horizontal component of Shearer's global image dataset. Two-D deconvolution has passed less noise and produced fewer artificial lineups. ray1-s2Dfx [ER]

noise than the two-dimensional deconvolution. This may be attributed to the greater degree of freedom FX-decon has in making predictions and to the extended length of the filter in the time domain.

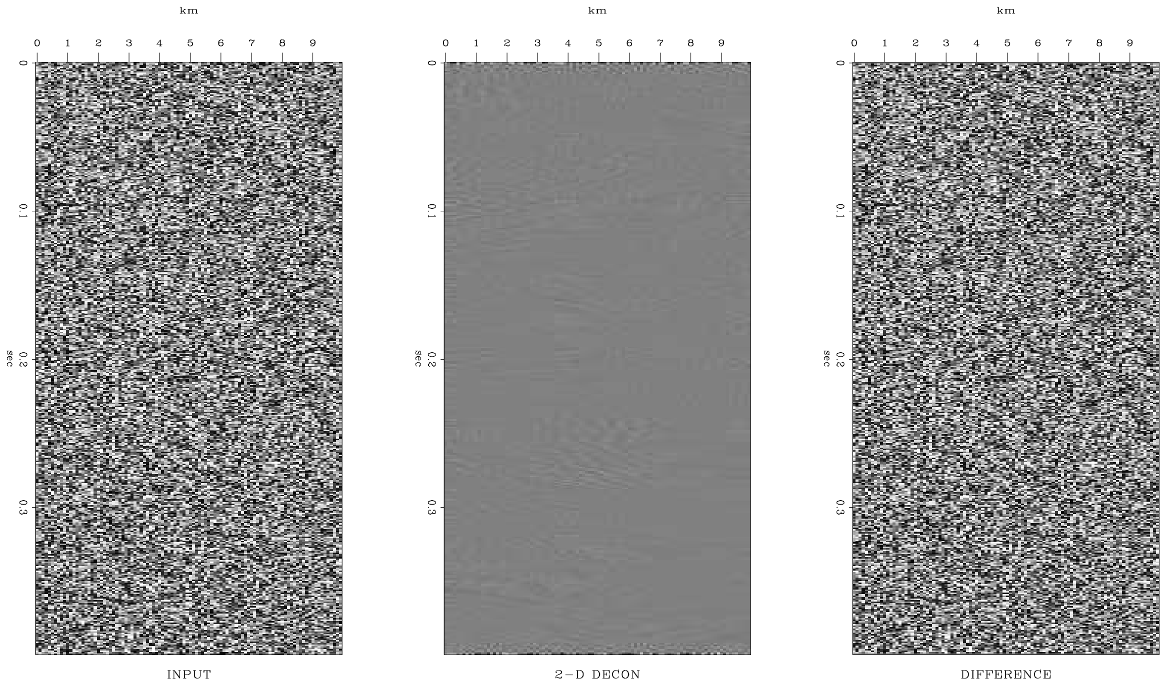

Figure 11: Random noise with two-D prediction filtering. There is less noise on output than seen in the comparable FX-decon output seen in Figure 12. ray1-rnoise [ER]

FX-decon applies a prediction process to each frequency separately, while two-dimensional prediction-error filtering generates a single filter for each window. Figures 13 and 14 show the results of creating three dipping events with a high-cut frequency of 15 Hz. and another three dipping events with a low-cut of 35 Hz. and a high-cut of 60 Hz. While some differences may be expected when applied to events with different frequency ranges, the differences between the results are found to be small.

Events with amplitudes that vary spatially, even in what seems to be a predictable manner, tend not to be predicted well by either technique. Figures 15 and 16 show the comparisons. The weak events seen following the events in Figure 15 are caused by the finite width of the filter and the zeroed background. The main energy in Figure 15 is the same as Figure 16. Here, FX-decon may be considered to have a slightly better prediction, but no major differences are seen.

CONCLUSIONS

FX-decon and two-dimensional deconvolution produce similar results with similar computer time requirements. The two-dimensional deconvolution filter might allow

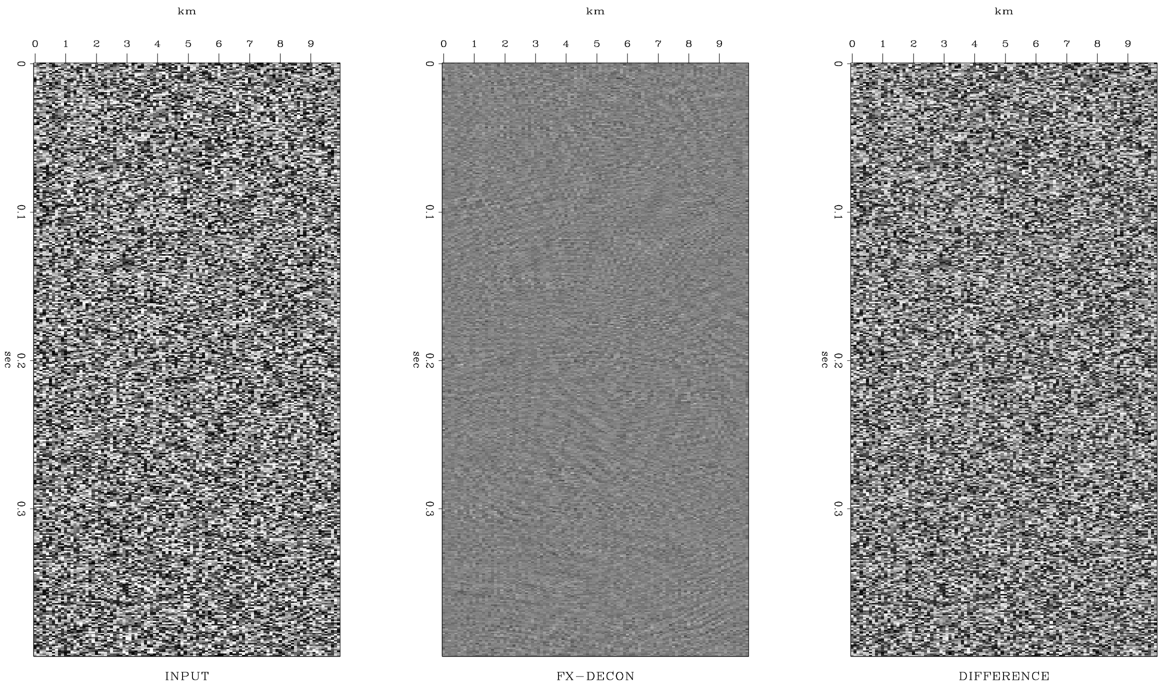

Figure 12: Random noise with FX-decon filtering. There is more noise on output than seen in the comparable two-D prediction filter output seen in Figure 11. ray1-rnoisefx [ER]

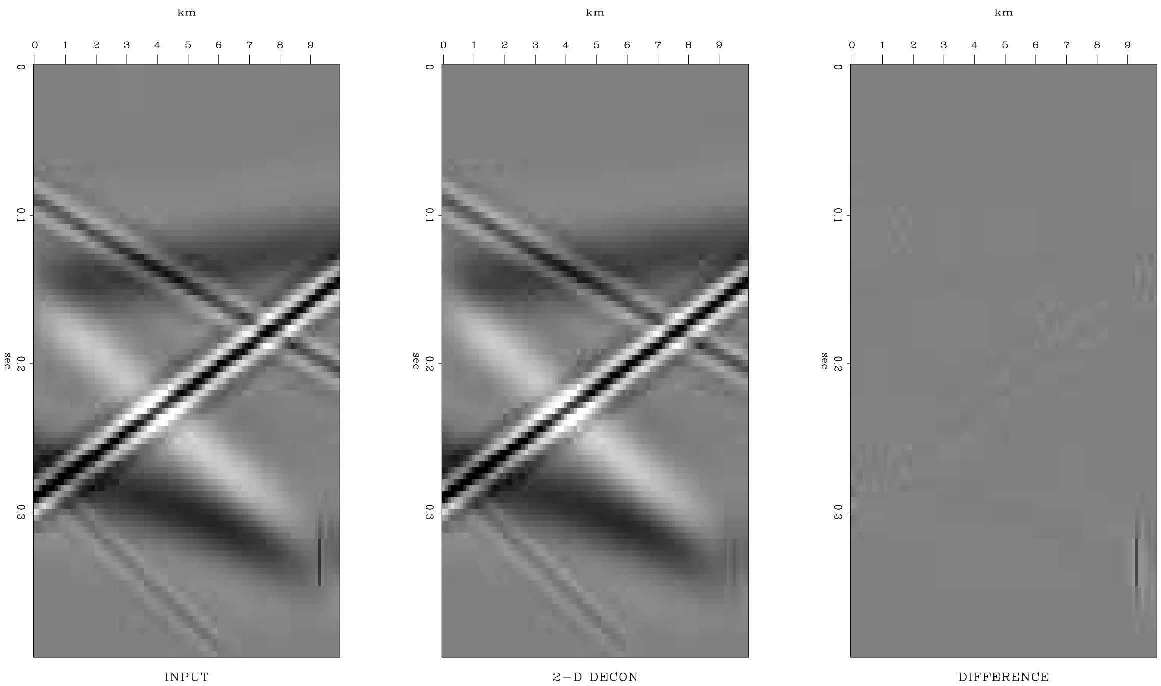

Figure 13: Dips of different frequency content with two-D prediction-error filtering ray1-fdips [ER]

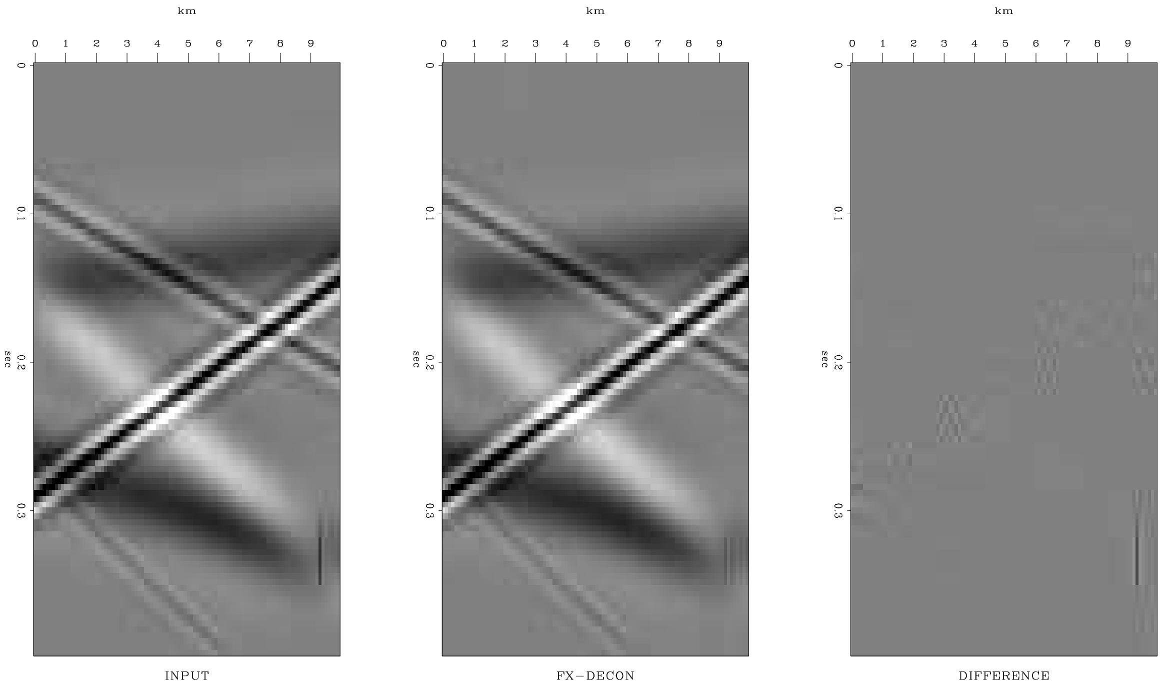

Figure 14: Dips of different frequency content with FX-decon filtering ray1-fdipsfx [ER]

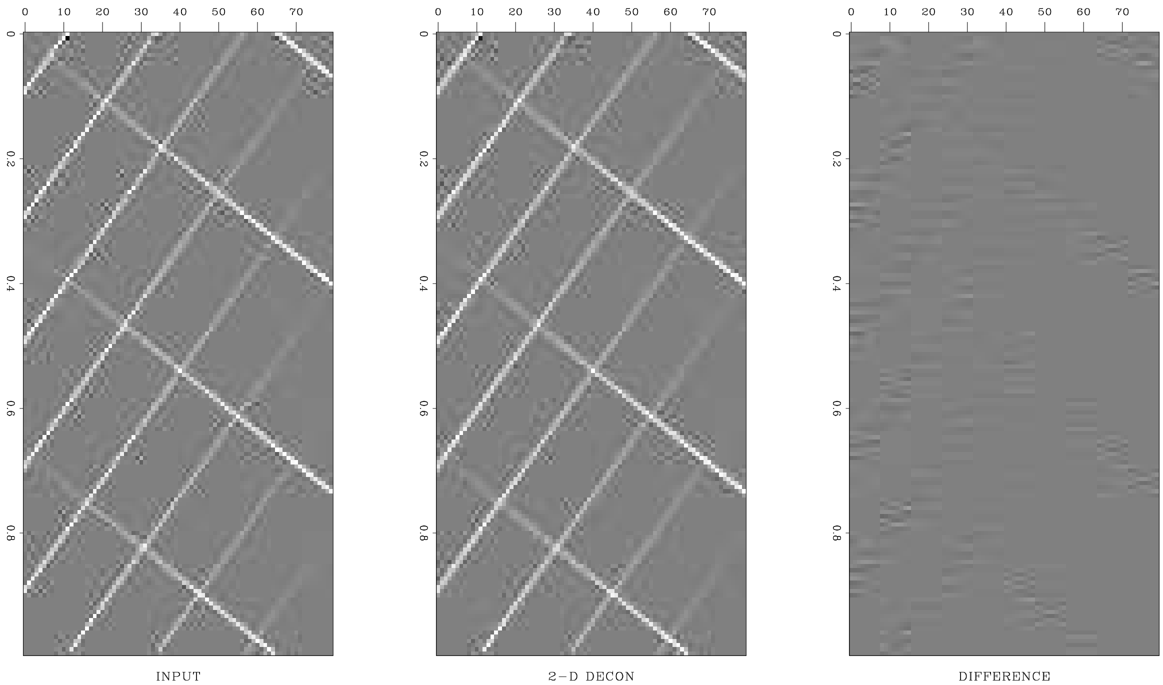

Figure 15: Two-D prediction-error filtering applied to conflicting events with changing amplitudes. ray1-conflict [ER]

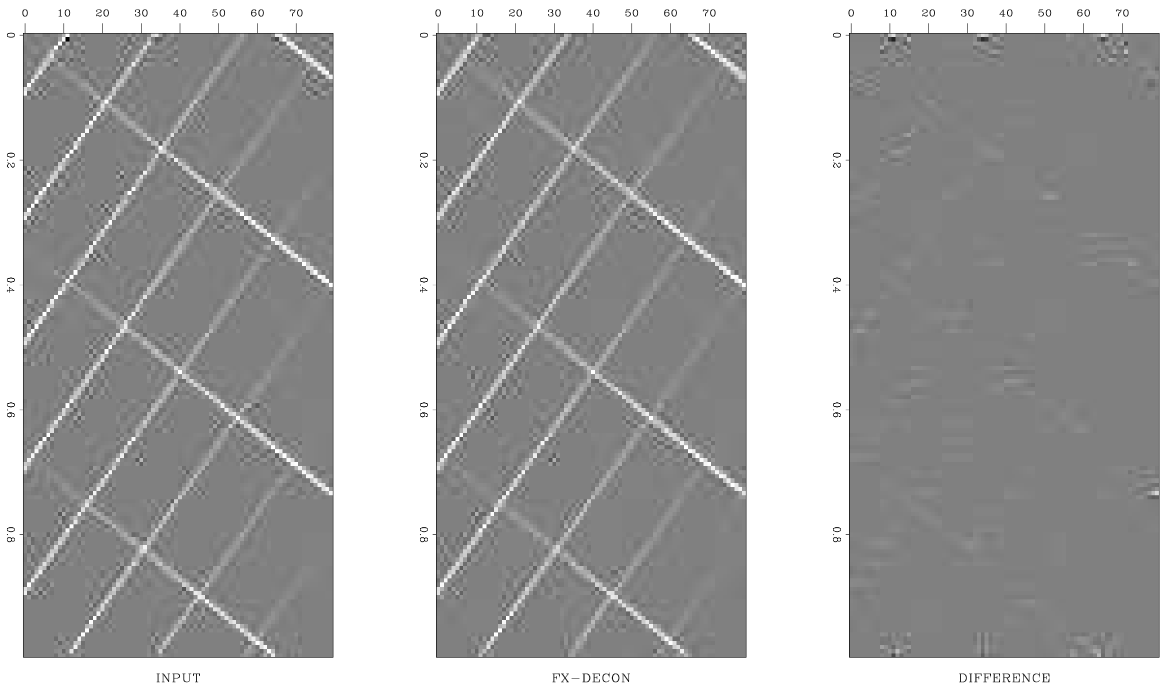

Figure 16: FX-decon filtering applied to conflicting events with changing amplitudes. ray1-conflictfx [ER]

more flexibility in controlling the action of the process than is allowed with FX-decon. For example, the range of dips passed by two-dimensional deconvolution might be controlled by the shape of the filter. Two-dimensional deconvolution appears to have some advantage over FX-decon since two-dimensional deconvolution does not produce the artificial lineups along strong signals to the extent FX-decon does. Two-dimensional deconvolution also does a better job of removing random noise.

REFERENCES

Abma, R., and Claerbout, J., 1993, Applications of Two-D deconvolution: SEP–**77**, 271–282.

Canales, L. L., 1984, Random noise reduction: 54th Annual Internat. Mtg., Soc. Expl. Geophys., Expanded Abstracts, Session:S10.1.

Claerbout, J. F., 1992a, Earth Soundings Analysis: Processing Versus Inversion: Blackwell Scientific Publications.

Claerbout, J. F., 1992b, Information from smiles: Mono-plane-annihilator weighted regression: SEP–**73**, 409–420.

Gulunay, N., 1986, Fx decon and complex wiener prediction filter: 56th Annual Internat. Mtg., Soc. Expl. Geophys., Expanded Abstracts, Session:POS2.10.

Shearer, P., 1991, Imaging global body wave phases by stacking long-period seismograms: Journal of Geophysical Research, **96**, 535–555.

Spitz, S., 1991, Seismic trace interpolation in the f-x domain: Geophysics, **56**, no. 6, 785–794.